Original Article

Extracellular vesicles derived from human dental pulp stem cells promote osteogenesis of adipose-derived stem cells via the MAPK pathway

Journal of Tissue Engineering
Volume 11: 1–14

DOI: 10.1177/2041731420975569
journals.sagepub.com/home/tej
SAGE

Qiaoqiao Jin[1,2*], Peilun Li[1,2*], Keyong Yuan[1,2], Fen Zhao[1,2], Xiaohan Zhu[1,2], Pengfei Zhang[1,2] and Zhengwei Huang[1,2]

Abstract

Recent studies have shown that co-culture systems play an important role in bone tissue engineering. In this study, human dental pulp stem cells (hDPSCs) were co-cultured with human adipose-derived stem cells (hADSCs), and osteoblastic phenotypes were found to be enhanced in co-cultures compared with monocultures of hDPSCs or hADSCs. Furthermore, GW4869, an inhibitor of extracellular vesicle (EV) formation, suppressed the mineralization of co-cultured cells. Studies indicate that the therapeutic potential of DPSCs is realized through paracrine action, in which EVs play an important role. To study their role, we successfully obtained and identified hDPSC-derived extracellular vesicles (hDPSC-EVs), and further investigated their effects on hADSCs and the underlying mechanism. hADSCs were stimulated with hDPSC-EVs, which were found to promote the migration and mineralization of hADSCs. Moreover, hDPSC-EVs promoted osteogenic differentiation by enhancing the phosphorylation of ERK 1/2 and JNK in hADSCs. To investigate the specific proteins in EVs that might play a role in hADSC osteogenic differentiation, we performed proteomic analysis of hDPSC-EVs. We determined the top 30 enriched pathways, which notably included the insulin signaling pathway. The number of genes enriched in the insulin signaling pathway was the largest, in addition to the "protein processing in endoplasmic reticulum" term. The MAPK cascade is a typical downstream pathway mediating insulin signaling. To further study the effects of hDPSC-EVs on maxillofacial bone regeneration, we used hDPSC-EVs as a cell-free biomaterial in a model of mandibular defects in rats. To assess the therapeutic potential of EVs, we analyzed their proteome. Animal experiments demonstrated that hDPSC-EVs promoted the regeneration of bone defects. Overall, these results highlight the potential of hDPSC-EVs to induce lineage specific differentiation of hADSCs. The results also indicated the importance of considering hDPSC-EVs as biomimetic materials for clinical translation of treatments for oral maxillofacial defects.

Keywords

Dental pulp stem cells, adipose-derived stem cells, co-culture, extracellular vesicles, bone regeneration

Received: 18 August 2020; accepted: 2 November 2020

Introduction

Stem cell-based bone tissue engineering is currently the most common method for repairing maxillofacial bone defects.[1] Human adipose-derived stem cells (hADSCs) harvested from liposuction procedures have been found to be an alternative cell source for clinical application because of their abundance and availability, and the low morbidity and discomfort during liposuction.[2] The osteogenic potential of hADSCs has been demonstrated in animal models and clinical trials.[3] However, challenges still

[1]Department of Endodontics, Ninth People's Hospital, College of Stomatology, Shanghai Jiao Tong University School of Medicine, Shanghai, China
[2]National Clinical Research Center for Oral Diseases, Shanghai Key Laboratory of Stomatology & Shanghai Research Institute of Stomatology, Shanghai, China

*Qiaoqiao Jin and Peilun Li contributed equally to the work.

Corresponding author:
Zhengwei Huang, Department of Endodontics, Ninth People's Hospital, College of Stomatology, Shanghai Jiao Tong University School of Medicine, 639 Zhizaoju Road, Shanghai 200011, P.R. China.
Email: huangzhengwei@shsmu.edu.cn

remain in the use of mesenchymal stem cells (MSCs) alone to repair bone tissues. The specialized differentiation of MSCs requires induction by the surrounding microenvironment, such as specific growth factors and extracellular matrix.[4] Certain growth factors are also required for the differentiation of hADSCs.[5] Reliable and predictable induction of specific differentiation of MSCs is key in bone tissue engineering applications.

Cytokines regulating cell differentiation alter cell fate and can be used to positively influence cell therapy outcomes.[6] Cell co-culture systems take advantage of this ability to promote tissue regeneration and repair.[7] MSCs themselves secrete large amounts of cytokines, including growth factors and chemokines.[8] Human dental pulp stem cells (hDPSCs) are thought to derive from the neural crest.[9] hDPSCs secrete multiple growth factors, which have been reported to be involved in the osteogenic differentiation of MSCs.[4] Therefore, this study investigated whether hDPSCs could be used to create an osteo-inductive niche that enhances the osteogenesis of hADSCs in co-culture.

Recently, extracellular vesicles (EVs) have been demonstrated to be the primary paracrine executor of stem cells.[10] EVs are micro-vesicles that are secreted by cells and facilitate intercellular communication.[11] EVs can travel between cells and deliver functional cargoes, such as proteins and RNAs, thereby regulating the differentiation, commitment, function, and proliferation of targeted cells.[12] Consequently, we speculated that hDPSCs might play an important role in regulating the osteogenic differentiation of hADSCs by secreting EVs. Mitogen-activated protein kinase (MAPK) signaling plays a complex and important regulatory role in osteogenesis.[13] The MAPK family includes three distinctly regulated groups: p38, extracellular signal-regulated kinase (ERK 1/2), and c-Jun N-terminal kinase (JNK).[14] Several in vitro studies have suggested that ERK 1/2 and JNK signaling pathways play an important role in cell osteogenic differentiation. Treatment with a ERK 1/2 or JNK inhibitor blocks osteoblast differentiation of ADSCs.[15,16]

In this study, hDPSCs were co-cultured with hADSCs to investigate whether hDPSCs could provide a microenvironment to facilitate hADSC differentiation. Next, hDPSCs were preincubated with GW4869, an inhibitor of EVs formation, to test whether hDPSC-derived EVs (hDPSC-EVs) might influence the osteogenic differentiation of hADSCs. In addition, hDPSC-EVs were extracted by ultracentrifugation, and the roles of hDPSC-EVs and their mechanisms in regulating the osteogenic differentiation ability of hADSCs were investigated in vitro. Furthermore, the extracted hDPSC-EVs were applied to a mandibular defect in rats to examine their effects on maxillofacial bone regeneration.

Materials and methods

Isolation and co-culture of hDPSCs and hADSCs

Impacted third molars were collected from six healthy patients. Subcutaneous adipose tissues were harvested from the abdomen of five healthy female patients who underwent liposuction. This study was approved by the Ethics Committee of Shanghai Ninth People's Hospital affiliated with Shanghai Jiao Tong University, School of Medicine China (Document No. 201769). All patients agreed to participate in the study and provided signed informed consent forms. To obtain stem cells, we followed the methods described previously.[17,18] For in vitro co-cultures, a mixture hDPSCs and hADSCs were cultured in osteoblast-inducing medium (OM) (Cyagen, Santa Clara, CA, USA) at ratios of 1:0, 1:1, and 0:1.

Osteogenic differentiation

To compare the osteogenic differentiation ability of co-cultured hDPSCs and hADSCs, we conducted alkaline phosphate (ALP) staining, ALP activity assays, and calcium deposition assays (Alizarin Red S staining, AL/ARS), as previously described.[19] For ALP staining, the cells were treated with OM for 1 week to induce osteogenesis, then fixed and stained with an ALP kit (Beyotime, Shanghai, China) according to the manufacturer's instructions. For ALP activity assays, after treatment with OM for 1 week, cells were incubated with p-nitrophenyl phosphate (Sigma-Aldrich, St. Louis, MO, USA), and activity was detected by measurement of optical density (OD) at 405 nm. The total protein content of the cells was also measured with a BCA (bicinchoninic acid) Protein Assay Kit (Pierce Biotechnology, Thermo Fisher Scientific, Waltham, MA, USA), and the ALP activity was expressed as OD per milligram of total protein. To measure mineralization, we cultured the cells in OM for 3 weeks to induce osteogenesis, then fixed them in 4% paraformaldehyde for 30 min and stained them with 2% Alizarin Red S (Sigma-Aldrich).

Quantitative real-time polymerase chain reaction (qRT-PCR)

Total RNA was extracted using TRIzol reagent (Invitrogen, Carlsbad, CA, USA), and cDNA was synthesized from total RNA using a PrimeScript RT reagent kit (Takara Bio, Inc. Shiga, Japan) as described previously.[19] Expression of mineralization markers: bone morphogenetic proteins (*BMP2*), *runt*-related transcription factor 2 (*RUNX2*) was assessed using SYBR Premix Ex Taq II (Takara Bio, Inc.), and gene expression was analyzed using a LightCycler 480 II (Roche, Mannheim, Germany). The primers are listed in Online Appendix1. Relative gene expression level was

analyzed according to the comparative Cq method[20] and normalized to GAPDH. All PCR amplifications were performed in triplicate.

Isolation and identification of hDPSC-EVs

After reaching 80% confluence in 10 cm^2 cell culture dishes, hDPSCs were rinsed three times with phosphate-buffered saline (PBS) and cultured with serum-free medium for 48 h. The culture supernatant was collected for further isolation and purification of EVs. HDPSC-EVs were collected from the supernatant by ultracentrifugation, as previously described.[21] Briefly, culture supernatants of hDPSCs were centrifuged at 4°C for 15 min at 300×*g* and at 4°C for another 15 min at 2000×*g* to eliminate cell debris. The supernatant was centrifuged at 4°C for 30 min at 10,000×*g* to remove dead cells and condensed with an ultra-filtration conical tube (Amicon Ultra-15, Millipore, Burlington, MA), then centrifuged at 4°C for 70 min at 100,000×*g*. Isolated EVs were rinsed with PBS and ultracentrifuged at 100,000×*g* for 70 min at 4°C. The suspensions were normalized to the hDPSC number from the culture plate from which they were isolated, then diluted so that 100 μL of suspension contained EVs isolated from 10 million hDPSCs. The hDPSC-EV concentration was detected with a BCA Protein Assay Kit (Thermo Fisher Scientific, Rockford, USA). The morphology of hDPSC-EVs was observed by transmission electron microscopy (TEM), as previously described.[22] TEM was used to identify the presence of hDPSC-EVs; 50 μL of a 1 in 100 dilution of exosome suspension (equivalent to EVs isolated from 50,000 cells) was placed on TEM grids and incubated for 30 min. The grids were then washed, dried, and imaged with a Hitachi H7500 transmission electron microscope (HITACHI, Japan) to identify the morphology of EVs. The size and concentration of hDPSC-EVs were determined by nanoparticle tracking analysis (NTA), and the results were analyzed with NTA analytical software (Zeta View, version 8.04.02) according to the manufacturer's instructions.[23,24] Through NTA, the particles were automatically tracked and sized according to their Brownian motion and the diffusion coefficient. HDPSC-EVs were diluted 1000-fold with PBS (equivalent to EVs isolated from 10,000 cells), then added into the nanopore instrument for measurement. Markers of EVs—CD9, CD63, CD81 and TSG101—were detected by western blotting to characterize hDPSC-EVs.

Cell migration assay

HADSC migration assays were performed as previously described.[25] The migration ability of hADSCs was assessed with Transwell inserts, which were 6.5 mm in diameter, with a pore size of 8 μm (Corning Inc. Corning, NY, USA), according to the manufacturer's protocol. hADSCs were seeded at a density of 2×10^4 cells/well into the upper chambers, with 200 μL serum-free DMEM, whereas 800 μL growth medium (GM) with 10% FBS containing hDPSC-EVs at different concentrations (0 μg/mL, 10 μg/mL, 20 μg/mL, and 40 μg/mL) was added to the lower chambers. After culture for 24 h, the chamber was gently washed by PBS. For removal of the non-migrated cells, the upper side of the membrane was wiped with a cotton swab. Then, the membranes were fixed with 4% paraformaldehyde and stained with 0.5% crystal violet for 10 min. The number of migrated cells was counted in five randomly selected microscopic fields per filter.

Exosome-mediated stem cell differentiation in vitro

To evaluate the effect of hDPSC-EVs on osteogenic differentiation of hADSCs, we performed ALP staining, ALP activity assays, qRT-PCR and immunofluorescence assays (IFAs) of RUNX2 and osteocalcin (OCN), as previously described.[26,27] The following four groups were assessed: (1) hADSCs cultured in osteoblast-inducing medium (OM) (Cyagen, Santa Clara, CA, USA) alone (0 μg/mL); (2) hADSCs cultured in OM supplemented with 10 μg/mL hDPSC-EVs (10 μg/mL); (3) hADSCs cultured in OM supplemented with 20 μg/mL hDPSC-EVs (20 μg/mL); and (4) hADSCs cultured in OM supplemented with 40 μg/mL hDPSC-EVs (40 μg/mL). The medium was renewed every 3 days. The experimental procedures of ALP staining, ALP activity assays, and qRT-PCR were performed as described above ("Osteogenic differentiation"; "Quantitative real-time polymerase chain reaction (qRT-PCR)"). For IFAs, the cytoskeleton was stained with fluorescein isothiocyanate (FITC)-phalloidin (Yeasen, China), and cellular nuclei were counterstained with 4′,6-diamidino-2-phenylindole (DAPI) (Sigma, USA). For the detection of RUNX2 and OCN expression, cells were fixed after 7 days of culture in OM with or without hDPSC-EVs (40 μg/mL). HADSCs were fixed were sequentially incubated with primary antibodies against RUNX2 (1:1600, Cell Signaling Technology) and OCN (1:1600, Cell Signaling Technology) overnight at 4°C. The next day, cells were incubated with the secondary antibody DyLight 549-conjugated anti-rabbit IgG antibody (Invitrogen, Carlsbad, CA, USA).

MAPK signaling pathway detection

Selective inhibitors of MAPK—SB203580 (SB, inhibitor of P38), PD98059 (PD, inhibitor of ERK 1/2), and SP600125 (SP, inhibitor of JNK) (all from Abcam, Cambridge, MA, USA)—were used to assess the participation of the MAPK signaling pathway in the hDPSC-EV-mediated effects on hADSCs.[28] The following five groups were assessed: (1) hADSCs cultured in OM alone (control); (2) hADSCs cultured in OM supplemented with

40 μg/mL hDPSC-EVs (EV); (3) hADSCs cultured in OM supplemented with 40 μg/mL hDPSC-EVs and 20 μg/μL SB203580 (SB); (4) hADSCs cultured in OM supplemented with 40 μg/mL hDPSC-EVs and 5 μg/μL PD98059 (PD); and (5) hADSCs cultured in OM supplemented with 40 μg/mL hDPSC-EVs and 5 μg/μL SP600125 (SP). The medium was renewed every 3 days. After hADSCs were incubated for 7 days, the osteogenic differentiation ability of hADSCs among different groups was evaluated by ALP staining. To detect the activation state of the MAPK signaling pathway, we first serum-starved hADSCs for 12 h and then treated them with 40 μg/mL hDPSC-EVs for 0, 10, 20, 30, or 60 min before they were harvested for western blot analysis.

Western blotting

Western blotting was conducted to analyze the expression of EV-related markers and the expression of phosphorylated P38, ERK1/2, and JNK proteins, as previously described.[29] The following primary antibodies were used: anti-CD9, anti-CD63, anti-CD81, anti-TSG101 (all from Abcam), rabbit anti-P38 MAPK (P38), anti-phospho-P38 (p-P38), anti-P44/42 MAPK (ERK1/2), anti-phospho-P44/42 MAPK (p-ERK 1/2), anti-JNK, anti-phospho-SAPK/JNK (p-JNK), and mouse anti-GAPDH. The secondary antibodies were HRP-conjugated goat anti-rabbit IgG and HRP-conjugated goat anti-mouse IgG (all from Cell Signaling Technology, Danvers, MA, USA).

HDPSC-EV proteomics

For proteomic analysis of hDPSC-EVs, we digested proteins with the filter-aided sample preparation protocol.[30] Briefly, protein samples were dissolved in 50 mM DTT, 50 mM Tris-HCl (pH 8.5), and 4% SDS, and centrifuged (10 min, 14,000×*g*). Approximately 100 μg of protein was diluted in 8 M urea in 0.1 M Tris-HCl, pH 8.5 (UA), then loaded onto 30 k filtration units (Microcon; Millipore). The denaturation buffer was replaced by washing three times with UA. The proteins were then alkylated with 50 mM iodoacetamide in UA (20 min, room temperature, in darkness), and the excess alkylation reagents were eliminated by washing three times with UA and three additional times with 50 mM NH_4HCO_3. Proteins were digested overnight with trypsin (V5111; Promega, Madison, WI, USA) in 50 mM NH_4HCO_3 at 37°C. The resulting peptides were eluted by centrifugation with 50 mM NH_4HCO_3 (twice) and 0.5 M NaCl. Trifluoroacetic acid was added to a concentration of 1%, and the peptides were finally desalted and dried down for further analysis. Subsequently, peptides were loaded onto the LC-MS/MS system. LC-MS/MS analysis was performed with an Ultimate 3000 RSLCnano system coupled online to a QExactive mass spectrometer (both from Thermo Scientific, Bremen, Germany). Approximately 500 ng of peptides was loaded onto the column, eluted for 75 min, and preconcentrated on a trap column (Acclaim PepMap 100, C18, 3 μm, 100 A, 150 μm × 20 mm). Next, the peptides were separated on an analytical column (Acclaim PepMap RSLC, C18, 1.9 μm, 100 A, 150 μm × 50 mm) with a gradient from 5% to 100% solvent B over 75 min (solvent A: 0.1% FA, solvent B: 0.1% FA, 80% ACN; flow rate 600 nL/min). Label-free quantification of proteins was performed via the iBAQ[31] method in Scaffold Viewer (Proteome Software). Briefly, precursor ion intensities of peptides matching those for each particular protein were divided by the theoretical number of peptides that could be derived from each particular protein by trypsin digestion. Gene Ontology (GO) enrichment analysis was evaluated with the GO Consortium website (http://www.geneontology.org/), and the Kyoto Encyclopedia of Genes and Genomes (KEGG) pathway database was used to annotate and classify the pathways of differentially expressed proteins. A p-value < 0.05 was chosen to select only significant categories.[32]

In vivo experiments in a rat mandible defect model

A prospective randomized controlled animal model design was adopted according to all recommendations of the ARRIVE guidelines (Animal Research: Reporting In Vivo Experiments). Procedures for rat mandibular bone defect models were performed as described previously.[33] All animal experiments were approved by the Animal Experimental Ethical Inspection committee of the Shanghai Ninth People's Hospital affiliated with Shanghai Jiao Tong University, School of Medicine, and were conducted according to the institutional animal guidelines. The operation was performed under general anesthesia with an intraperitoneal ketamine (10% 100 mg/kg) injection. Articaine (Ultracaine DS, 3M ESPE; 0.5 mL) was additionally injected subcutaneously and into the masseter muscle for local anesthesia and control of bleeding. The animals were maintained under anesthesia during the entire surgical procedure. After local disinfection (Betadine 10%, Egis, Hungary), an incision in the skin was made, and masseter muscle dissection was performed. Mandibular defects were created (2 mm diameter) with a 2-mm burr (Hager & Meisinger GmbH, Neuss, Germany) in the area of mandibular angle. Emerging studies suggest that the self-assembling peptide hydrogel PuraMatrix™ may facilitate bone regeneration in bone defects.[34,35] Here, we used PuraMatrix as a scaffold material to carry hDPSC-EVs. The sites were divided into three groups: (1) 50 μL 1% PuraMatrix™ (3-D Matrix, Ltd., Tokyo, Japan) alone (control); (2) 50 μL 1% PuraMatrix™/40 μg/mL hDPSC-EV complex; and (3) 50 μL 1% PuraMatrix™/4000 μg/mL hDPSC-EV complex. After the defect was made, the hydrogel scaffold material was injected and sutured. The rats

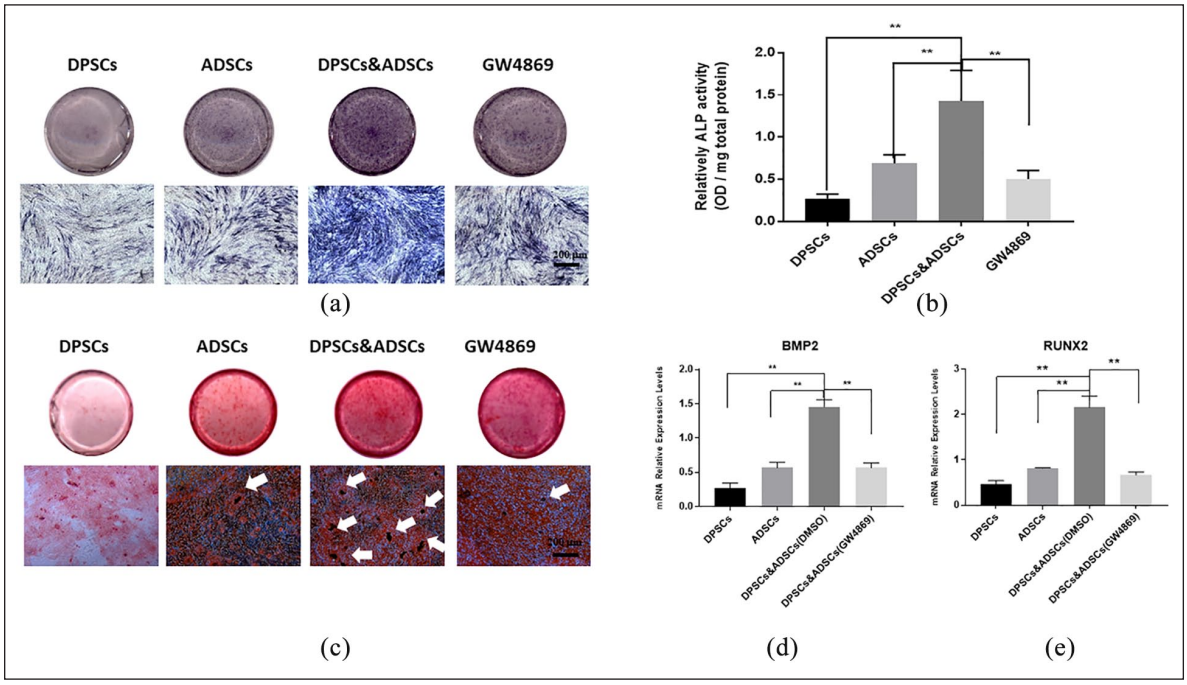

Figure 1. HDPSCs improved the osteogenic differentiation of hADSCs, probably via EVs. HDPSCs and hADSCs were co-cultured in the presence of GW4869 or DMSO. (a) ALP staining of the co-cultured hDPSCs and hADSCs. (b) Quantitative analysis of ALP activity in the co-cultured hDPSCs and hADSCs. (c) Alizarin Red S staining of the co-cultured hDPSCs and hADSCs. Calcium nodules are indicated by white arrows. (d, e) PCR detection of BMP2 and RUNX2 expression involved in osteogenic differentiation of co-cultured hDPSCs and hADSCs. Data are presented as the mean ± standard deviation of the mean ($n = 3$), * represents $p < 0.05$, ** represents $p < 0.01$.

were intraperitoneally administered Alizarin Red S (AL), tetracycline hydrochloride (TE), and calcein (CA) (all from Sigma-Aldrich) at 1 week, 3 weeks, and 5 weeks after the operation, respectively. All animals were sacrificed at week 6, and the paraformaldehyde-fixed tissue specimens were scanned with a micro-computed tomography instrument (Micro-CT, SkyScan 1176; BrukerOptik GmbH, Belgium). The bone volume/total volume (BV/TV), mean trabecular separation (Tb.Sp), mean trabecular number (Tb.N), and mean trabecular thickness (Tb.Th) were calculated as previously described.[36] Thereafter, the polymethylmethacrylate-embedded specimens were sectioned into 50 μm thick slices with a saw microtome (Leica, Nussloch, Germany). Sequential fluorescence labeling of the specimens was observed under a confocal laser scanning microscope (CLSM 700; Carl Zeiss, Oberkochen, Germany).[27] Van Gieson's picro-fuchsin staining was used for histological analysis, and the measurements on the specimens were performed with a personal computer-based image analysis system (image-Pro PlusTM, Media Cybernetics, Silver Spring, MD, USA).[37] A schematic images of animal experiments in the Online Appendix 1.

Statistical analysis

All data are presented as the mean ± standard deviation of at least three independent repeated experiments. Data were evaluated with Student's *t* tests and one-way analysis of variance followed by Tukey's multiple comparisons test (Prism 6.0). $p < 0.05$ was considered to indicate a statistically significant difference.

Results

HDPSCs mediate osteogenic differentiation of hADSCs via EVs

The results of ALP staining and activity assay showed that co-cultures of hDPSCs and hADSCs displayed stronger ALP activity (Figure 1(a) and (b)) than hDPSCs or hADSCs cultured alone. In addition, the results of Alizarin Red staining were consistent with the ALP activity. More calcium nodules were observed in the co-cultures (white arrow, Figure 1(c)) than in either the hDPSCs or hADSCs cultured alone. qRT-PCR indicated that co-cultures of hDPSCs and hADSCs expressed higher levels of *BMP2* and *RUNX2* than hDPSCs or hADSCs cultured alone (Figure 1(d) and (e)). Together, these results suggested that osteoblastic phenotypes were enhanced in co-cultures compared with monocultures of hDPSCs or hADSCs. To examine whether EVs were involved in promoting osteogenic differentiation of hADSCs in the co-culture system, we added GW4869 to the co-culture system.[38] The addition of GW4869 significantly decreased the ALP activity

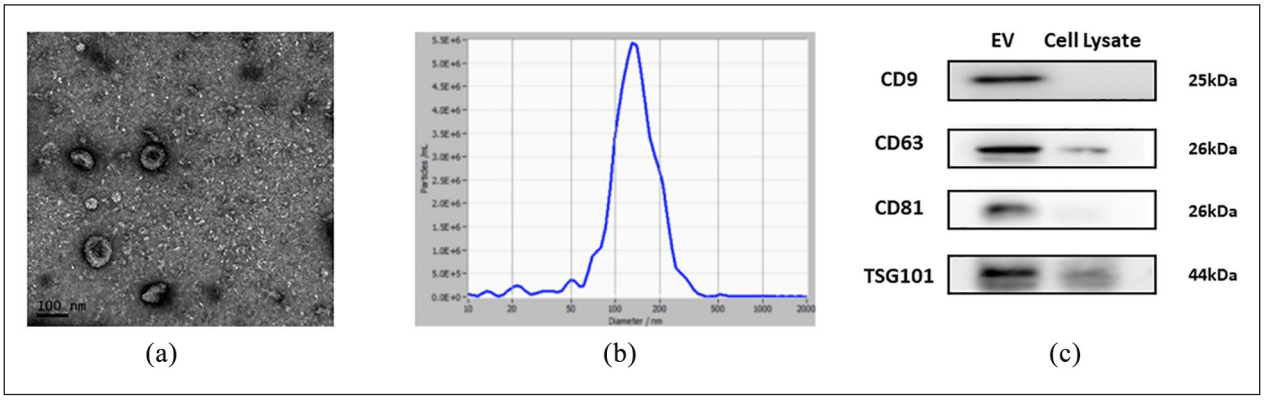

Figure 2. Characteristics of hDPSC-EVs. (a) TEM observation of hDPSC-EVs; (b) particle size identification of hDPSC-EVs detected by NTA; (c) western blotting analysis of CD9, CD63, CD81, and TSG101 in EVs.

and calcium nodule formation in the co-culture group (Figure 1(a)–(c)). Meanwhile, blocking exosome secretion also diminished the expression of osteogenic genes (*BMP2* and *RUNX2*) in the co-culture group (Figure 1(d) and (e)).

Characterization of hDPSC-EVs

To directly investigate the roles of hDPSC-EVs, we extracted and identified hDPSC-EVs. TEM revealed the cup-shaped appearance of hDPSC-EVs, with a diameter of approximately 100 nm (Figure 2(a)). NTA analysis revealed that the main peak of nanoparticles, which covered 80% of isolated EVs, ranged mainly from 76.5 to 202.5 nm. The mean size ± SD of exosomes was 138.7 ± 68 nm (Figure 1(c)), corresponding to the size distribution of EVs reported previously[39,40] (Figure 2(b)). Western blotting analysis demonstrated that hDPSC-EVs expressed several EV proteins: CD9, CD63, CD81, and TSG101 (Figure 2(c)).

HDPSC-EVs promote the migration and osteogenic differentiation of hADSCs

To explore the effects of hDPSC-EVs on hADSCs, we treated hADSCs with different concentrations of hDPSC-EVs, and observed the migration and differentiation of hADSCs. Previous studies have assessed the role of ADSCs in bone regeneration and tissue repair by examining their migration ability.[26] First, we found that the migration ability of hADSCs markedly improved after the addition of hDPSC-EVs, as compared with that of negative controls ($p < 0.05$ or $p < 0.01$, Figure 3(a) and (b)). For osteogenic differentiation of hADSCs, ALP staining and quantification revealed that when the loading of hDPSC-EVs was 10–40 μg/mL, ALP expression in the hADSCs was significantly upregulated ($p < 0.05$ or $p < 0.01$, Figure 3(c) and (d)). The optimal concentration of EVs to promote osteogenic differentiation of hADSCs was 40 μg/mL. Meanwhile, the mRNA levels of osteoblastic marker genes (*BMP2* and *RUNX2*) were also significantly up-regulated ($p < 0.05$ or $p < 0.01$, Figure 3(e) and (f)). The RUNX2 and OCN immunofluorescence detection results further confirmed the osteogenic induction potential of hDPSC-EV on hADSCs in vitro (Figure 3(g) and (h)).

HDPSC-EVs activate the MAPK pathway in hADSC, thus, promoting osteogenic differentiation

MAPK signaling pathway inhibition assays and western blotting were performed to analyze the activation state of the MAPK signaling pathway. As to the evaluation of MAPK pathway, hDPSC-EVs supplemented with the p38 MAPK inhibitor SB203580 (SB), the ERK MAPK inhibitor PD98059 (PD), and the JNK MAPK inhibitor SP600125 (SP). As shown in Figure 4(a) and (b), after the addition of PD or SP, the osteogenic differentiation ability of hADSCs induced by hDPSC-EVs was clearly weaker than that in the EV group ($p < 0.01$). In contrast, no significant difference in the osteogenic ability of hADSCs was observed between the SB group and the EV group (Figure 4(a) and (b)). To further explore the role of the MAPK pathway in EV-mediated osteogenic differentiation of hADSCs, we conducted western blot assays to evaluate the protein levels of p-p38, and p38, p-ERK 1/2, ERK 1/2 1/2, p-JNK, and JNK in the MAPK pathway (Figure 4(c)–(e)). According to the ratio of intensities, p-P38/P38 decreased dramatically at 10 min ($p < 0.01$), whereas the ratios of p-ERK 1/2/ERK 1/2 and p-JNK/JNK increased dramatically at 10 min ($p < 0.01$, Figure 4(f)–(h)).

Proteomics of the hDPSC-EVs

Proteomics analysis of the hDPSC-EVs identified 3565 proteins implicated in three global functions such as cellular components, biological processes, or molecular functions (GO terms). GO analysis tests whether a particular set of genes is enriched in certain GO terms. The top 30 GO enrichment terms identified are shown in Figure 5(a). hDPSC-EVs were enriched in glycolysis pathways, cytoskeletal GTPases,

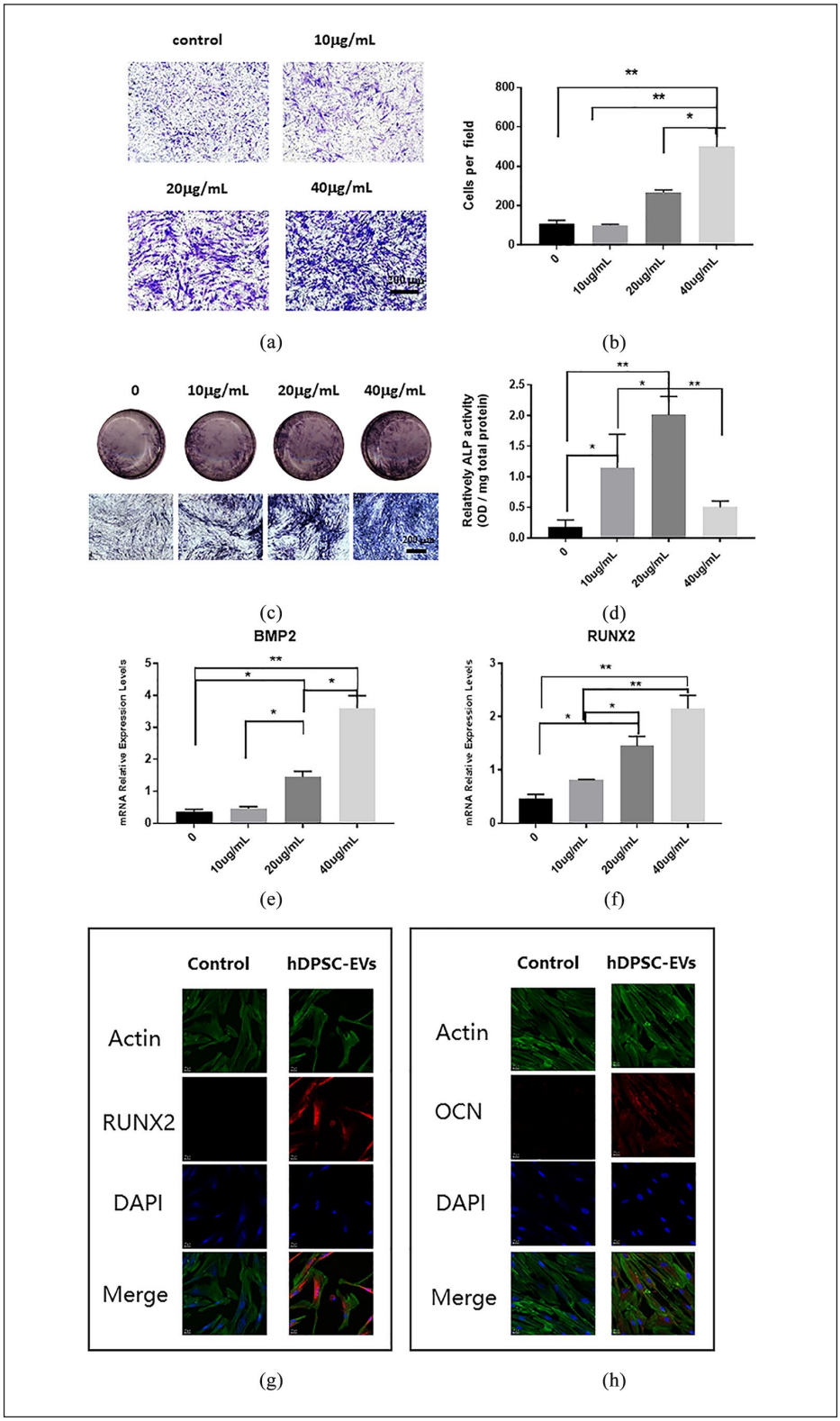

Figure 3. The effects of hDPSC-EVs on the migration and osteogenic differentiation of hADSCs. (a) Transwell migration assay to detect the effect of hDPSC-EVs on the migration of hADSCs. (b) Quantitative analysis of the effects of hDPSC-EVs on the migration of hADSCs. (c) ALP staining to detect the effect of hDPSC-EVs on osteogenic differentiation of hADSCs. (d) Quantitative detection of ALP activity to detect the effects of hDPSC-EVs on osteogenic differentiation of hADSCs. (e, f) The effects of hDPSC-EVs on the expression of the osteogenic-related genes RUNX2 and BMP2 in hADSCs. (g, h) Immunofluorescence detection of RUNX2 and OCN expression in hADSCs after 7 days incubation with 40 μg/mL hDPSC-EVs. Data are presented as the mean ± standard deviation of the mean ($n = 3$), * represents $p < 0.05$, ** represents $p < 0.01$.

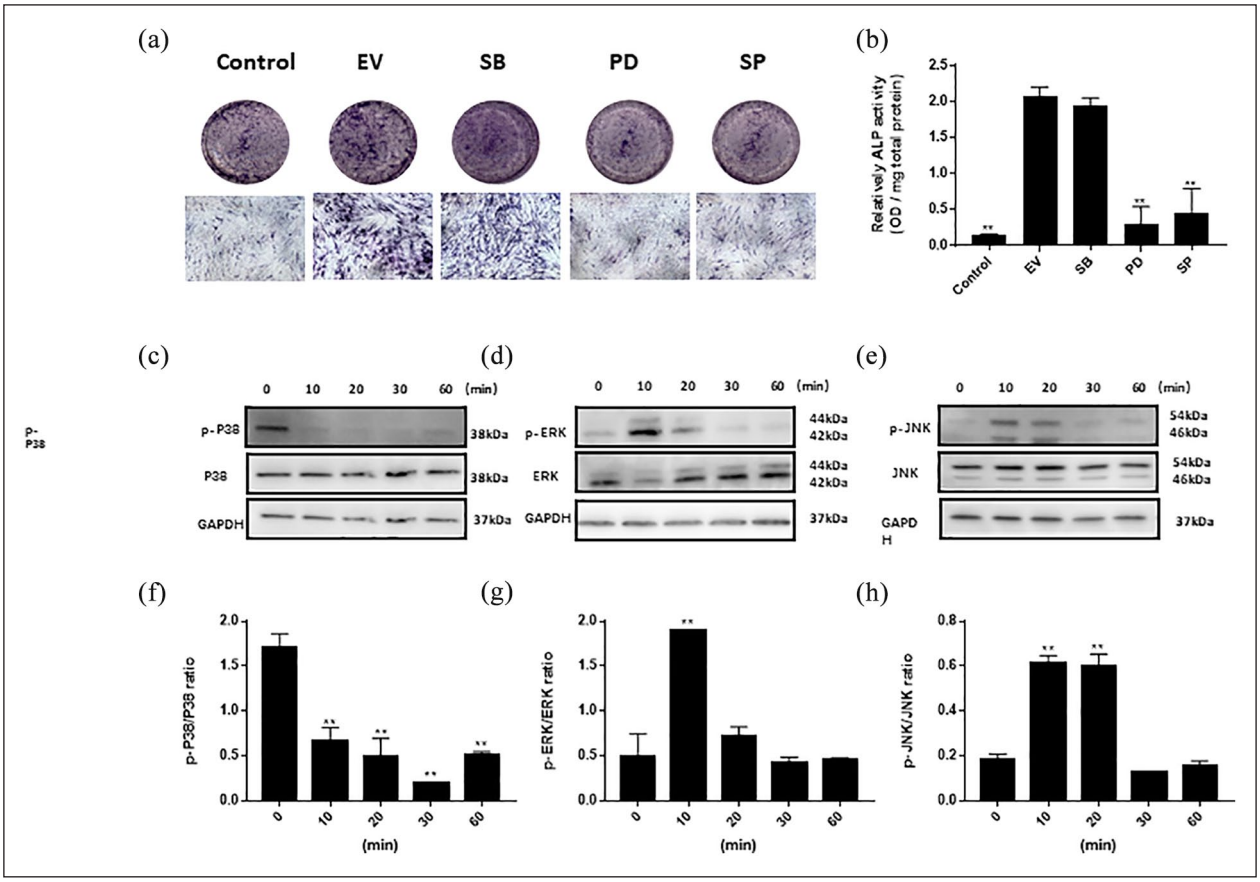

Figure 4. Effects of hDPSC-EVs on the MAPK pathway in hADSCs. (a) ALP staining of hADSCs after treatment with hDPSC-EVs and/or inhibitors. (b) Quantitative detection of ALP activity of hADSCs treated with hDPSCEVs and/or inhibitors. (c–e) Protein expression of p-P38/P38, p-ERK 1/2 1/2/ERK 1/2, and p-JNK/JNK, determined by western blotting. (f–h) The ratios of p-P38/P38, p-ERK 1/2 1/2/p-ERK 1/2, and p-JNK/JNK intensity. SB: SB203580, inhibitor of P38; PD: PD98059, inhibitor of ERK 1/2; and SP: SP600125, inhibitor of JNK. Data are presented as the mean ± standard deviation of the mean ($n = 3$), ** represents $p < 0.01$.

and signal recognition (Figure 5(a)), which were characteristic of EVs (mesenchymal stem cell exosome: a novel stem cell-based therapy for cardiovascular disease; mesenchymal stem cell exosome ameliorates reperfusion injury through proteomic complementation). To determine which signaling pathways might contribute to the osteogenic differentiation of hADSCs regulated by exogenous proteins, we performed KEGG pathway analysis and listed the top 30 KEGG enrichment pathways (Figure 5(b)). Interestingly, in addition to the term "protein processing in endoplasmic reticulum" (p value=7.958e−11), the number of genes enriched in the insulin signaling pathway (p value=2.289e−06) was largest. Moreover, proteins associated with the MAPK pathway—MAPK1 (ERK2), MAPK3 (ERK1), MAPK8 (JNK1), MAPK9 (JNK2), and MAPK10 (JNK3)—were also enriched in the insulin signaling pathway.

HDPSC-EVs mediate bone regeneration in vivo

As shown in Figure 6(a), the micro-CT images revealed that both the high-dose and low-dose groups had much greater quantities of new bone than the control group (Figure 6(a)). According to quantitative evaluation of the newly formed bone within each region of interest (Figure 6(b)–(e)), the BV/TV, Tb.N, and Tb.Sp were all significantly higher in both the high and low-dose group than in the control group. Furthermore, according to sequential fluorescence labeling, visible new bone formation and mineralization occurred in the high-dose group as early as the first week after implantation, whereas the low-dose group exhibited clear new bone formation in the third week. Only weak calcium deposition was observed in the control group. During the fifth week, bone formation increased slightly in the control group, but was still significantly slower than that in the high-dose or the low-dose group (Figure 6(f) and (g)). However, no significant difference was observed in the amount of new bone formation between the high-dose group and the low-dose group at week 3 or 5. Histological sections of regions of interest are presented in Figure 6(h). The apposition of new bone in the high-dose and low-dose groups was greater than that in the control group, in which only a small amount of new

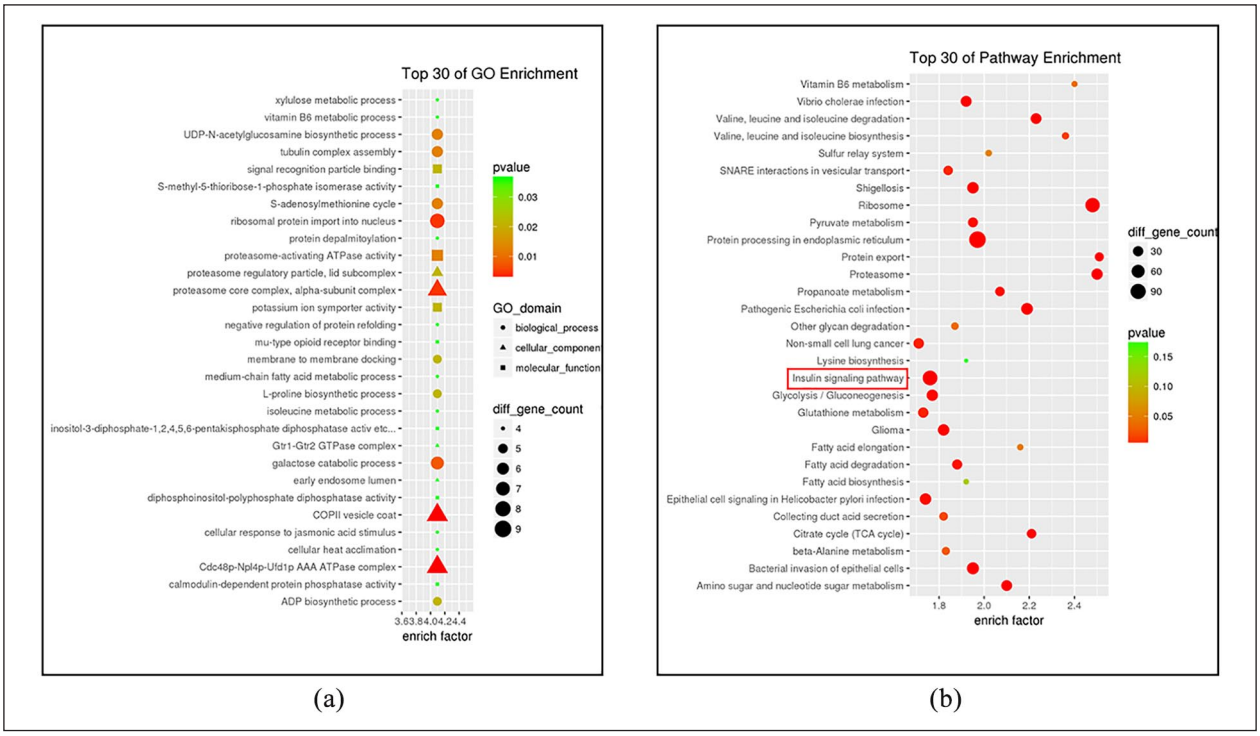

Figure 5. Analysis of the protein profile of hDPSC-EVs. (a) Top 30 Gene Ontology functional pathway enrichment terms. (b) Top 30 KEGG pathway enrichment terms of proteins derived from hDPSC-EVs.

bone was formed (Figure 6(h)). Quantitative histomorphometric analysis revealed significant differences between the experimental group and the control group ($p < 0.05$ or $p < 0.01$, Figure 6(i)).

Discussion

HADSCs have been shown to be a promising and appealing source of MSCs for BTE due to their abundance, the fact that they are less invasive to harvest, and their efficient growth in culture.[41] Accumulating research have proven that hADSCs are highly sensitive to the culture environment, which may affect their osteogenic differentiation.[42] Previous in vitro studies verified the superior osteogenesis of BMSCs compared to ADSCs[43]; however, controversy remains over which cells exhibit better osteogenic differentiation potential in vivo.[44] Therefore, we speculated that environmental factors may be important for osteogenic differentiation of ADSCs. The co-culture system has recently gained particular attention in bone tissue engineering, and inspiring outcomes have been observed.[45] This novel approach is considered to be a less costly strategy than adding particular growth factors into the culture medium. Previous reports have revealed the importance of cell–cell interactions in inducing their specific differentiation.[26,46] Studies have shown that in the absence of exogenous growth factors, paracrine factors released by helper cells in the co-culture system can regulate the pluripotent differentiation of target cells to promote tissue metabolism, homeostasis and repair.[47] Therefore, a co-culture system may construct a suitable microenvironment for hADSCs.

HDPSCs are usually originate from the neural crest, which have great potential ability of multi-directional differentiation, and studies have shown that stem cells can perform their biological functions by secreting a variety of growth factors.[48] However, it is important to note that when compared to hADSCs, the source of hDPSCs can' t be guaranteed, since not all clinical patients can provide healthy, caries-free wisdom teeth. In this study, hADSCs were co-cultured with hDPSCs to investigate whether hDPSCs could enhance the osteogenic potential of hADSCs by regulating the intercellular communication. This study produced the encouraging results that hDPSCs could provide an osteo-inductive microenvironment to promote the osteogenic capacity of hADSCs. This result may indicate that different cell types can take advantage of the naturally-occurring cross-talk in a co-culture environment. Previous studies have proved that EVs are the primary mediator that regulate intercellular communication,[11] therefore this study examined whether hDPSCs might regulate hADSCs via EVs. The results further verified the hypothesis by applying an inhibitor of EVs (GW4869). The results showed that EVs derived from hDPSCs regulated the osteogenic differentiation ability of hADSCs to a certain extent. However, the precise regulatory effects of

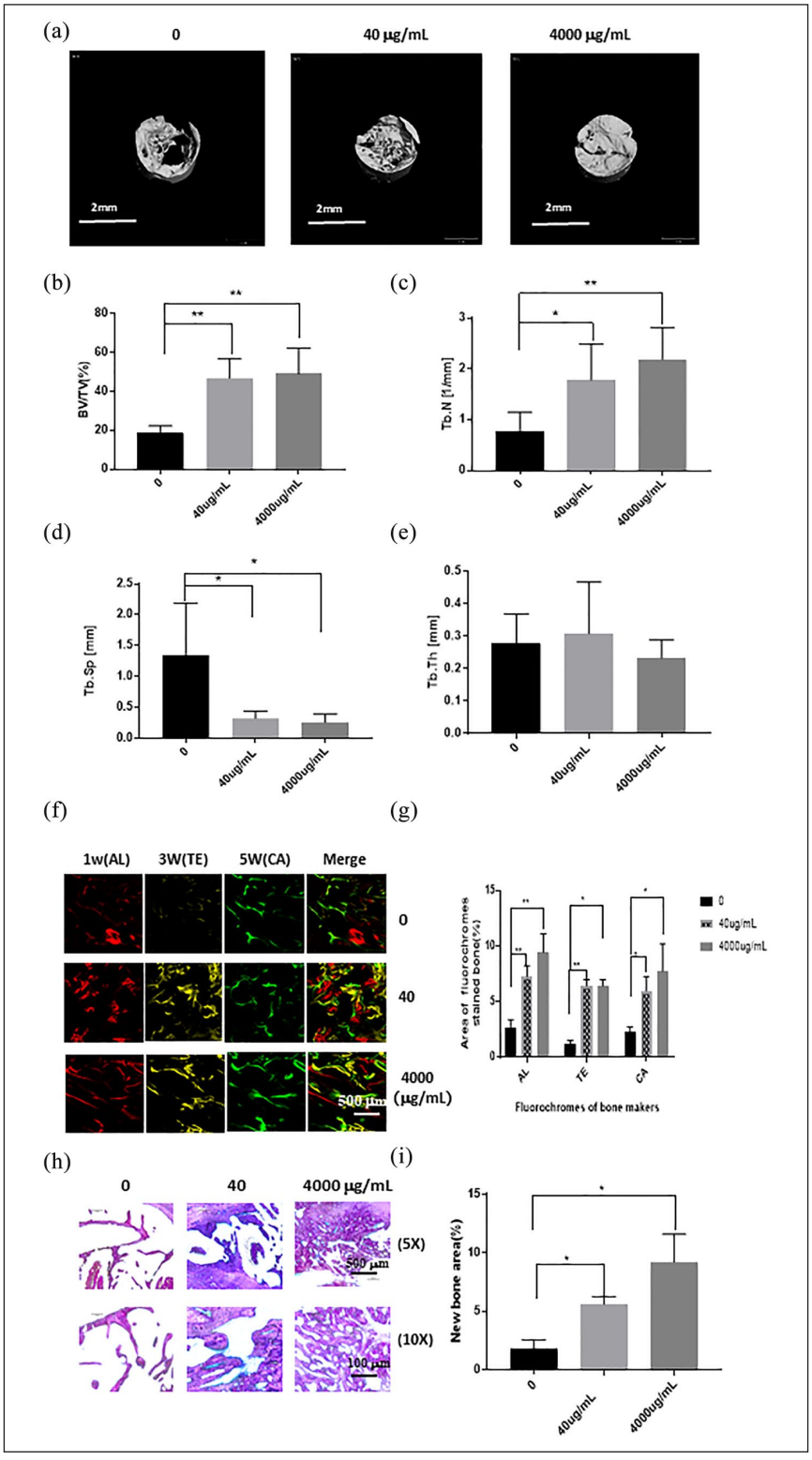

Figure 6. The effects of hDPSC-EVs on osteogenic ability were analyzed by micro-CT, confocal laser scanning microscopy, and histological staining. (a) Micro-CT images taken at 6 weeks after implantation. (b) Bone volume/total volume (BV/TV), (c) trabecular number (Tb.N), (d) trabecular thickness (Tb.Th), and (e) trabecular separation (Tb.Sp), analyzed by micro-CT for each group at 6 weeks after implantation. (f) Alizarin Red S (AL), tetracycline hydrochloride (TE), and calcein (CA) were used for sequential fluorescence labeling at 1, 3, and 5 weeks after implantation. (g) The percentage of TE, AL, and CA fluorescence labeling in each group, assessed at week 6 after implantation. (h) Histological staining of the sample stained with Van Gieson's picro-fuchsin. (i) The percentage of new bone area, assessed at 6 weeks after implantation by histomorphometric analysis. Data are presented as the mean ± standard deviation of the mean ($n = 3$), * represents $p < 0.05$, ** represents $p < 0.01$.

hDPSC-EVs on hADSCs remains unclear. Given this, a series of in vitro experiments were conducted to investigate whether hDPSC-EVs could be used as a biomolecule to regulate hADSCs. In vitro studies revealed that the hDPSC-EVs could markedly improve the migration capacity of hADSCs. Previous studies have assessed the roles of ADSCs in bone regeneration and tissue repair by examining their migration ability.[49,50] Here, we found that the osteogenic ability of hADSCs significantly increased in the presence of hDPSC-EVs. These findings illustrated that hDPSC-EVs strongly affect hADSCs and may accelerate their osteogenic ability. Thus, the combination of hDPSC-EVs and hADSCs may serve as an alternative effective treatment for maxillofacial bone defects.

MAPKs are key players in bone development and skeletal homeostasis, particularly in osteoblast differentiation. EVs have been found to increase the proliferation of osteoblasts and MSCs through the MAPK pathway.[51] The role of P38-MAPK signaling in TGF-β1-mediated osteogenesis has been described in rat ADSCs,[52] and osteo-induction of hADSCs has been associated with ERK 1/2/JNK signaling.[53] In view of the characteristics of hDPSC-EVs and the important role of the MAPK signaling pathway in osteogenic differentiation of stem cells, we conducted a series of studies to explore the links among hDPSC-EVs, the promotion of osteogenic differentiation of hADSCs, and MAPK signaling. After the addition of selective inhibitors of ERK 1/2 and JNK pathways, the effect of hDPSC-EVs in promoting osteogenic differentiation of hADSCs significantly decreased. However, selective inhibitors of the P38 pathway did not influence the EV effects. After hADSCs were treated with hDPSC-EVs, the expression of proteins in the ERK 1/2 and JNK pathway increased in hADSCs. However, compared with that in the control group, the expression of the phosphorylated P38 protein in hADSCs was significantly inhibited after the addition of hDPSC-EVs. These results indicated that the effects of hDPSC-EVs on hADSC osteogenesis of are partly mediated through the ERK 1/2 and JNK MAPK signaling pathways. ERK 1/2 has been associated with cell growth and osteogenic-related gene expression, whereas JNK is associated with cell growth arrest, apoptosis, and differentiation.[54,55] Although P38 is critical for different cellular functions, the influence of P38 pathways on osteogenic differentiation has been a matter of controversy.[56–58] However, little disagreement appears to exist regarding the effects of the ERK 1/2 or JNK pathway on stem cell differentiation.[59]

EVs have been studied comprehensively in disease therapy and tissue regeneration because of their roles in cell-to-cell signaling communication.[11] EVs can transfer bioactive molecules such as proteins, miRNAs and lipids, and play a pluripotent role in target cells.[60] Moreover, EVs exhibit low immunogenicity because they do not contain MHC molecules.[61,62] Mardpour et al.[63] found that chemoattractant proteins in the MSC-EV proteome—such as CXCL2, CXCL8, CXCL16, HERC5, IFITM2, and DEFA1, which recruits immune cells to injury sites—may enhance the immune response and inhibit the progression of infectious diseases. Liao et al.[64] have found that BMSC-EVs carrying microRNA-122-5p promote proliferation of osteoblasts via RTK/Ras/MAPK signaling pathway. Astrocyte-derived EV-transported miR-34c has been found to promote the proliferation of neuroblastoma cells by downregulating the NF-κB/MAPK axis.[65] Moreover, Li et al.[66] have found that human keratinocyte-derived EV miRNA-21 significantly promotes the healing of skin wounds by activating the ERK signaling pathway. Oral mesenchymal cell derived-EVs have attracted attention because of their good performance in the treatment of multiple diseases, such as in stimulating angiogenesis,[21] alleviating lung inflammatory reactions,[67] and promoting skin wound healing.[68] The GO results showed that hDPSC-EVs are enriched in glycolytic pathways, and studies have shown that glycolysis-related enzymes in MSC-EV can be used to mitigate reperfusion injury in an animal model of myocardial ischemia/reperfusion injury.[62] To study the specific proteins in hDPSC-EVs that may influence the osteogenic differentiation of hADSCs, we performed a KEGG analysis of hDPSC-EVs proteomics. Most hDPSC-EV proteins are involved in protein synthesis, protein processing, and the insulin signaling pathway. In the past, the insulin signaling pathway was primarily associated with glucose metabolism. However, in recent years, studies increasingly indicate roles of this signaling pathway in angiogenesis and osteogenesis.[69,70] The MAPK pathway is a canonical downstream pathway in insulin signaling.[71] In KEGG analysis, the MAPK pathway-related proteins enriched in the insulin signaling pathway included ERK1/2 and JNK, in agreement with the results of our study on the pathways of osteogenic differentiation from hDPSC-EVs to hADSCs in vitro. Moreover, the IGF/MAPK axis has been reported previously to promote the differentiation of human dental pulp stem cells.[72] However, the effects of the insulin-MAPK signaling axis in osteogenesis requires further research, and the hDPSC-EV derived proteins that play a role in osteogenesis require experimental detection and verification. Furthermore, this study investigated whether hDPSC-EVs, as cell-free biomaterials, might promote bone regeneration in the absence of exogenous stem cells. The results of animal experiments demonstrated that the hDPSC-EVs alone promoted the repair of mandibular defects in rats, probably by mobilizing the endogenous stem cells to bone defect sites.

In summary, this study demonstrated that hDPSCs enhance the osteogenic differentiation of hADSCs during co-culture. HDPSC-EVs improved the migration ability of hADSCs. In addition, the MAPK pathway may be involved in promoting osteogenic differentiation of hADSCs by hDPSC-EVs. Protein profile results suggest that the insulin-MAPK signaling axis may play a role in the regulation of hDPSC-EVs. Such study lays a foundation for further

research of the key proteins derived from hDPSC-EVs. Further investigation is required to characterize the mechanisms by which EVs mediate their therapeutic effects and the key proteins that contribute to this process. Moreover, our investigations provide important insights into the osteoinductive ability of hDPSC-EVs. These data solidify the paracrine effects of MSCs on bone repair, and suggest the importance of hDPSC-EVs in both endogenous bone regeneration as well as in maxillofacial tissue engineering.

Author contributions

Qiaoqiao Jin, Peilun Li, contributed to conception, design, data acquisition, analysis, and interpretation, drafted and revised the manuscript; Zhengwei Huang, contributed to conception, design, and data interpretation, drafted and critically revised the manuscript; Keyong Yuan, Xiaohan Zhu, contributed to data acquisition, drafted and revised the manuscript; Fen Zhao, Pengfei Zhang, contributed to data analysis and interpretation, drafted and revised the manuscript. All authors gave final approval and agree to be accountable for all aspects of the work.

Declaration of conflicting interests

The author(s) declared no potential conflicts of interest with respect to the research, authorship, and/or publication of this article.

Funding

The author(s) disclosed receipt of the following financial support for the research, authorship, and/or publication of this article: This work was supported by grants from the National Natural Science Foundation of China (No. 81570964 & No. 82071104), and was partly supported by the Shanghai's top priority clinical medicine center (No. 2017ZZ01011).

ORCID iD

Zhengwei Huang https://orcid.org/0000-0001-9861-514X

Supplemental material

Supplemental material for this article is available online.

References

1. Wu V, Helder MN, Bravenboer N, et al. Bone tissue regeneration in the oral and maxillofacial region: a review on the application of stem cells and new strategies to improve vascularization. *Stem Cells Int* 2019; 2019: 6279721.
2. Storti G, Scioli MG, Kim BS, et al. Adipose-derived stem cells in bone tissue engineering: useful tools with new applications. *Stem Cells Int* 2019; 2019: 3673857.
3. Sándor GK, Numminen J, Wolff J, et al. Adipose stem cells used to reconstruct 13 cases with cranio-maxillofacial hard-tissue defects. *Stem Cells Transl Med* 2014; 3(4): 530–540.
4. Vidane AS, Zomer HD, Oliveira BM, et al. Reproductive stem cell differentiation: extracellular matrix, tissue microenvironment, and growth factors direct the mesenchymal stem cell lineage commitment. *Reprod Sci (Thousand Oaks, Calif)* 2013; 20(10): 1137–1143.
5. Carbone A, Valente M, Annacontini L, et al. Adipose-derived mesenchymal stromal (stem) cells differentiate to osteoblast and chondroblast lineages upon incubation with conditioned media from dental pulp stem cell-derived osteoblasts and auricle cartilage chondrocytes. *J Biol Regul Homeostatic Agents* 2016; 30(1): 111–122.
6. Pourrajab F, Babaei Zarch M, Baghi Yazdi M, et al. Application of stem cell/growth factor system, as a multimodal therapy approach in regenerative medicine to improve cell therapy yields. *Int J Cardiol* 2014; 173(1): 12–19.
7. Hubka KM, Dahlin RL, Meretoja VV, et al. Enhancing chondrogenic phenotype for cartilage tissue engineering: monoculture and coculture of articular chondrocytes and mesenchymal stem cells. *Tissue Eng Part B Rev* 2014; 20(6): 641–654.
8. Drago D, Cossetti C, Iraci N, et al. The stem cell secretome and its role in brain repair. *Biochimie* 2013; 95(12): 2271–2285.
9. Janebodin K, Horst OV, Ieronimakis N, et al. Isolation and characterization of neural crest-derived stem cells from dental pulp of neonatal mice. *PLoS One* 2011; 6(11): e27526.
10. Deng H, Sun C, Sun Y, et al. Lipid, protein, and microrna composition within mesenchymal stem cell-derived exosomes. *Cell Reprogram* 2018; 20(3): 178–186.
11. Mathieu M, Martin-Jaular L, Lavieu G, et al. Specificities of secretion and uptake of exosomes and other extracellular vesicles for cell-to-cell communication. *Nat Cell Biol* 2019; 21(1): 9–17.
12. Yin K, Wang S and Zhao RC. Exosomes from mesenchymal stem/stromal cells: a new therapeutic paradigm. *Biomarker Res* 2019; 7: 8.
13. Greenblatt MB, Shim JH and Glimcher LH. Mitogen-activated protein kinase pathways in osteoblasts. *Annu Rev Cell Dev Biol* 2013; 29: 63–79.
14. Farooq A and Zhou MM. Structure and regulation of mapk phosphatases. *Cell Signal* 2004; 16(7): 769–779.
15. Jaiswal RK, Jaiswal N, Bruder SP, et al. Adult human mesenchymal stem cell differentiation to the osteogenic or adipogenic lineage is regulated by mitogen-activated protein kinase. *J Biol Chem* 2000; 275(13): 9645–9652.
16. Yu Y, Mu J, Fan Z, et al. Insulin-like growth factor 1 enhances the proliferation and osteogenic differentiation of human periodontal ligament stem cells via erk and jnk mapk pathways. *Histochem Cell Biol* 2012; 137(4): 513–525.
17. Lin W, Gao L, Jiang W, et al. The role of osteomodulin on osteo/odontogenic differentiation in human dental pulp stem cells. *BMC Oral Health* 2019; 19(1): 22.
18. Wang PY, Thissen H and Kingshott P. Stimulation of early osteochondral differentiation of human mesenchymal stem cells using binary colloidal crystals (BCCs). *ACS Appl Mater Interfaces* 2016; 8(7): 4477–4488.
19. Jin Q, Yuan K, Lin W, et al. Comparative characterization of mesenchymal stem cells from human dental pulp and adipose tissue for bone regeneration potential. *Artif Cells Nanomed Biotechnol* 2019; 47(1): 1577–1584.
20. Livak KJ and Schmittgen TD. Analysis of relative gene expression data using real-time quantitative PCR and the 2(-delta delta c(t)) method. *Methods (San Diego, Calif)* 2001; 25(4): 402–408.

21. Komaki M, Numata Y, Morioka C, et al. Exosomes of human placenta-derived mesenchymal stem cells stimulate angiogenesis. *Stem Cell Res Ther* 2017; 8(1): 219.
22. Tooi M, Komaki M, Morioka C, et al. Placenta mesenchymal stem cell derived exosomes confer plasticity on fibroblasts. *J Cell Biochem* 2016; 117(7): 1658–1670.
23. Sokolova V, Ludwig AK, Hornung S, et al. Characterisation of exosomes derived from human cells by nanoparticle tracking analysis and scanning electron microscopy. *Colloids Surf B Biointerfaces* 2011; 87(1): 146–150.
24. Szatanek R, Baj-Krzyworzeka M, Zimoch J, et al. The methods of choice for extracellular vesicles (EVS) characterization. *Int J Mol Sci* 2017; 18(6): 1153.
25. Li W, Liu Y, Zhang P, et al. Tissue-engineered bone immobilized with human adipose stem cells-derived exosomes promotes bone regeneration. *ACS Appl Mater Interfaces* 2018; 10(6): 5240–5254.
26. Chew JRJ, Chuah SJ, Teo KYW, et al. Mesenchymal stem cell exosomes enhance periodontal ligament cell functions and promote periodontal regeneration. *Acta Biomater* 2019; 89: 252–264.
27. Zhang W, Zhang X, Wang S, et al. Comparison of the use of adipose tissue-derived and bone marrow-derived stem cells for rapid bone regeneration. *J Dent Res* 2013; 92(12): 1136–1141.
28. Zhang Q, Wang J, Duan MT, et al. Nf-κb, erk, p38 mapk and jnk contribute to the initiation and/or maintenance of mechanical allodynia induced by tumor necrosis factor-alpha in the red nucleus. *Brain Res Bull* 2013; 99: 132–139.
29. Niu C, Yuan K, Ma R, et al. Gold nanoparticles promote osteogenic differentiation of human periodontal ligament stem cells via the p38 mapk signaling pathway. *Mol Med Rep* 2017; 16(4): 4879–4886.
30. Otero-Ortega L, Laso-García F, Gómez-de Frutos MD, et al. White matter repair after extracellular vesicles administration in an experimental animal model of subcortical stroke. *Sci Rep* 2017; 7: 44433.
31. Wilhelm M, Schlegl J, Hahne H, et al. Mass-spectrometry-based draft of the human proteome. *Nature* 2014; 509(7502): 582–587.
32. Wu X, Liu L, Li J, et al. Proteome analysis using iTRAQ reveals the differentiation between Tibetan and ordinary ovalbumin peptides. *Int J Biol Macromol* 2019; 132: 722–728.
33. Kustro T, Kiss T, Chernohorskyi D, et al. Quantification of the mandibular defect healing by micro-CT morphometric analysis in rats. *J Cranio-Maxillo-Facial Surg: Off Publ Eur Assoc Cranio-Maxillo-Facial Surg* 2018; 46(12): 2203–2213.
34. Misawa H, Kobayashi N, Soto-Gutierrez A, et al. Puramatrix facilitates bone regeneration in bone defects of calvaria in mice. *Cell Transplant* 2006; 15(10): 903–910.
35. Nakahara H, Misawa H, Yoshida A, et al. Bone repair using a hybrid scaffold of self-assembling peptide puramatrix and polyetheretherketone cage in rats. *Cell Transplant* 2010; 19(6): 791–797.
36. Su Y, Komasa S, Li P, et al. Synergistic effect of nanotopography and bioactive ions on peri-implant bone response. *Int J Nanomed* 2017; 12: 925–934.
37. Wang S, Zhang Z, Xia L, et al. Systematic evaluation of a tissue-engineered bone for maxillary sinus augmentation in large animal canine model. *Bone* 2010; 46(1): 91–100.
38. Sterzenbach U, Putz U, Low LH, et al. Engineered exosomes as vehicles for biologically active proteins. *Mol Ther: J Am Soc Gene Ther* 2017; 25(6): 1269–1278.
39. Feng N, Jia Y and Huang X. Exosomes from adipose-derived stem cells alleviate neural injury caused by microglia activation via suppressing nf-kb and mapk pathway. *J Neuroimmunol* 2019; 334: 576996.
40. Liu X, Yang Y, Li Y, et al. Integration of stem cell-derived exosomes with in situ hydrogel glue as a promising tissue patch for articular cartilage regeneration. *Nanoscale* 2017; 9(13): 4430–4438.
41. Nielsen E, Chen L, Hansen JO, et al. Optimizing osteogenic differentiation of ovine adipose-derived stem cells by osteogenic induction medium and fgfb, bmp2, or nell1 in vitro. *Stem Cells Int* 2018; 2018: 9781393.
42. Bacakova L, Zarubova J, Travnickova M, et al. Stem cells: their source, potency and use in regenerative therapies with focus on adipose-derived stem cells - a review. *Biotechnol Adv* 2018; 36(4): 1111–1126.
43. Shafiee A, Seyedjafari E, Soleimani M, et al. A comparison between osteogenic differentiation of human unrestricted somatic stem cells and mesenchymal stem cells from bone marrow and adipose tissue. *Biotechnol Lett* 2011; 33(6): 1257–1264.
44. Wen Y, Jiang B, Cui J, et al. Superior osteogenic capacity of different mesenchymal stem cells for bone tissue engineering. *Oral Surg Oral Med Oral pathol Oral Radiol* 2013; 116(5):e324–e332.
45. Liu Y, Chan JK and Teoh SH. Review of vascularised bone tissue-engineering strategies with a focus on co-culture systems. *J Tissue Eng Regener Med* 2015; 9(2): 85–105.
46. Djouad F, Delorme B, Maurice M, et al. Microenvironmental changes during differentiation of mesenchymal stem cells towards chondrocytes. *Arthritis Res Ther* 2007; 9(2): R33.
47. Wang Y, Chen X, Yin Y, et al. Human amnion-derived mesenchymal stem cells induced osteogenesis and angiogenesis in human adipose-derived stem cells via erk1/2 mapk signaling pathway. *BMB Rep* 2018; 51(4): 194–199.
48. Halim NS, Aizat WM and Yahaya BH. The effect of mesenchymal stem cell-secreted factors on airway epithelial repair. *Regener Med* 2019; 14(1): 15–31.
49. Liu X, Zhu W, Wang L, et al. Mir-145-5p suppresses osteogenic differentiation of adipose-derived stem cells by targeting semaphorin 3a. *In Vitro Cell Dev Biol Anim* 2019; 55(3): 189–202.
50. Zubkova ES, Beloglazova IB, Makarevich PI, et al. Regulation of adipose tissue stem cells angiogenic potential by tumor necrosis factor-alpha. *J Cell Biochem* 2016; 117(1): 180–196.
51. Zhao P, Xiao L, Peng J, et al. Exosomes derived from bone marrow mesenchymal stem cells improve osteoporosis through promoting osteoblast proliferation via mapk pathway. *Eur Rev Med Pharmacol Sci* 2018; 22(12): 3962–3970.
52. Liu Y, Zheng WK, Gao WS, et al. Function of tgf-beta and p38 makp signaling pathway in osteoblast differentiation from rat adipose-derived stem cells. *Eur Rev Med Pharmacol Sci* 2013; 17(12): 1611–1619.

53. Tsang EJ, Wu B and Zuk P. Mapk signaling has stage-dependent osteogenic effects on human adipose-derived stem cells in vitro. *Connective Tissue Res* 2018; 59(2): 129–146.
54. Simmons CA, Nikolovski J, Thornton AJ, et al. Mechanical stimulation and mitogen-activated protein kinase signaling independently regulate osteogenic differentiation and mineralization by calcifying vascular cells. *J Biomech* 2004; 37(10): 1531–1541.
55. Zhang P, Wu Y, Jiang Z, et al. Osteogenic response of mesenchymal stem cells to continuous mechanical strain is dependent on erk1/2-runx2 signaling. *Int J Mol Med* 2012; 29(6): 1083–1089.
56. Lee JS, Ha L, Park JH, et al. Mechanical stretch suppresses bmp4 induction of stem cell adipogenesis via upregulating erk but not through downregulating smad or p38. *Biochem Biophys Res Commun* 2012; 418(2): 278–283.
57. Ulsamer A, Ortuño MJ, Ruiz S, et al. Bmp-2 induces osterix expression through up-regulation of dlx5 and its phosphorylation by p38. *J Biol Chem* 2008; 283(7): 3816–3826.
58. Zhang P, Wu Y, Dai Q, et al. P38-mapk signaling pathway is not involved in osteogenic differentiation during early response of mesenchymal stem cells to continuous mechanical strain. *Mol Cell Biochem* 2013; 378(1–2): 19–28.
59. Mu C, Lv T, Wang Z, et al. Mechanical stress stimulates the osteo/odontoblastic differentiation of human stem cells from apical papilla via erk 1/2 and jnk mapk pathways. *BioMed Res Int* 2014; 2014: 494378.
60. Katsuda T and Ochiya T. Molecular signatures of mesenchymal stem cell-derived extracellular vesicle-mediated tissue repair. *Stem Cell Res Ther* 2015; 6: 212.
61. Lai RC, Arslan F, Lee MM, et al. Exosome secreted by MSC reduces myocardial ischemia/reperfusion injury. *Stem Cell Res* 2010; 4(3): 214–222.
62. Lai RC, Yeo RW, Tan KH, et al. Mesenchymal stem cell exosome ameliorates reperfusion injury through proteomic complementation. *Regener Med* 2013; 8(2): 197–209.
63. Mardpour S, Hamidieh AA, Taleahmad S, et al. Interaction between mesenchymal stromal cell-derived extracellular vesicles and immune cells by distinct protein content. *J Cell Physiol* 2019; 234(6): 8249–8258.
64. Liao W, Ning Y, Xu HJ, et al. Bmsc-derived exosomes carrying microrna-122-5p promote proliferation of osteoblasts in osteonecrosis of the femoral head. *Clin Sci (London, England: 1979)* 2019; 133(18): 1955–1975.
65. Wu W, Liu J, Yang C, et al. Astrocyte-derived exosome-transported microrna-34c is neuroprotective against cerebral ischemia/reperfusion injury via tlr7 and the nf-κb/mapk pathways. *Brain Res Bull* 2020; 163: 84–94.
66. Li Q, Zhao H, Chen W, et al. Human keratinocyte-derived microvesicle mirna-21 promotes skin wound healing in diabetic rats through facilitating fibroblast function and angiogenesis. *Int J Biochem Cell Biol* 2019; 114: 105570.
67. Monsel A, Zhu YG, Gudapati V, et al. Mesenchymal stem cell derived secretome and extracellular vesicles for acute lung injury and other inflammatory lung diseases. *Expert Opin Biol Ther* 2016; 16(7): 859–871.
68. He X, Dong Z, Cao Y, et al. MSC-derived exosome promotes m2 polarization and enhances cutaneous wound healing. *Stem Cells Int* 2019; 2019: 7132708.
69. Fang Y, Xue Z, Zhao L, et al. Calycosin stimulates the osteogenic differentiation of rat calvarial osteoblasts by activating the igf1r/pi3k/akt signaling pathway. *Cell Biol Int* 2019; 43(3): 323–332.
70. Zeng Y, Zhang L and Hu Z. Cerebral insulin, insulin signaling pathway, and brain angiogenesis. *Neurol Sci: Off J Ital Neurol Soc Ital Soc Clin Neurophysiol* 2016; 37(1): 9–16.
71. King GL, Park K and Li Q. Selective insulin resistance and the development of cardiovascular diseases in diabetes: the 2015 Edwin Bierman award lecture. *Diabetes* 2016; 65(6): 1462–1471.
72. Vandomme J, Touil Y, Ostyn P, et al. Insulin-like growth factor 1 receptor and p38 mitogen-activated protein kinase signals inversely regulate signal transducer and activator of transcription 3 activity to control human dental pulp stem cell quiescence, propagation, and differentiation. *Stem Cells Dev* 2014; 23(8): 839–851.